



Hybrid Bearing Prognostic Test Rig

Paula J. Dempsey
Glenn Research Center, Cleveland, Ohio

Joseph M. Certo and Robert F. Handschuh
U.S. Army Research Laboratory, Glenn Research Center, Cleveland, Ohio

Florin Dimofte
University of Toledo, Toledo, Ohio

The NASA STI Program Office . . . in Profile

Since its founding, NASA has been dedicated to the advancement of aeronautics and space science. The NASA Scientific and Technical Information (STI) Program Office plays a key part in helping NASA maintain this important role.

The NASA STI Program Office is operated by Langley Research Center, the Lead Center for NASA's scientific and technical information. The NASA STI Program Office provides access to the NASA STI Database, the largest collection of aeronautical and space science STI in the world. The Program Office is also NASA's institutional mechanism for disseminating the results of its research and development activities. These results are published by NASA in the NASA STI Report Series, which includes the following report types:

- **TECHNICAL PUBLICATION.** Reports of completed research or a major significant phase of research that present the results of NASA programs and include extensive data or theoretical analysis. Includes compilations of significant scientific and technical data and information deemed to be of continuing reference value. NASA's counterpart of peer-reviewed formal professional papers but has less stringent limitations on manuscript length and extent of graphic presentations.
- **TECHNICAL MEMORANDUM.** Scientific and technical findings that are preliminary or of specialized interest, e.g., quick release reports, working papers, and bibliographies that contain minimal annotation. Does not contain extensive analysis.
- **CONTRACTOR REPORT.** Scientific and technical findings by NASA-sponsored contractors and grantees.

- **CONFERENCE PUBLICATION.** Collected papers from scientific and technical conferences, symposia, seminars, or other meetings sponsored or cosponsored by NASA.
- **SPECIAL PUBLICATION.** Scientific, technical, or historical information from NASA programs, projects, and missions, often concerned with subjects having substantial public interest.
- **TECHNICAL TRANSLATION.** English-language translations of foreign scientific and technical material pertinent to NASA's mission.

Specialized services that complement the STI Program Office's diverse offerings include creating custom thesauri, building customized databases, organizing and publishing research results . . . even providing videos.

For more information about the NASA STI Program Office, see the following:

- Access the NASA STI Program Home Page at <http://www.sti.nasa.gov>
- E-mail your question via the Internet to help@sti.nasa.gov
- Fax your question to the NASA Access Help Desk at 301-621-0134
- Telephone the NASA Access Help Desk at 301-621-0390
- Write to:
NASA Access Help Desk
NASA Center for Aerospace Information
7121 Standard Drive
Hanover, MD 21076



Hybrid Bearing Prognostic Test Rig

Paula J. Dempsey
Glenn Research Center, Cleveland, Ohio

Joseph M. Certo and Robert F. Handschuh
U.S. Army Research Laboratory, Glenn Research Center, Cleveland, Ohio

Florin Dimofte
University of Toledo, Toledo, Ohio

Prepared for the
2005 Annual Meeting and Exhibition
sponsored by the Society of Tribologists and Lubrication Engineers
Las Vegas, Nevada, May 15–19, 2005

National Aeronautics and
Space Administration

Glenn Research Center

Available from

NASA Center for Aerospace Information
7121 Standard Drive
Hanover, MD 21076

National Technical Information Service
5285 Port Royal Road
Springfield, VA 22100

Available electronically at <http://gltrs.grc.nasa.gov>

Hybrid Bearing Prognostic Test Rig

Paula J. Dempsey
National Aeronautics and Space Administration
Glenn Research Center
Cleveland, Ohio 44135

Joseph M. Certo and Robert F. Handschuh
U.S. Army Research Laboratory
Glenn Research Center
Cleveland, Ohio 44135

Florin Dimofte
The University of Toledo
Toledo, Ohio 43606

Abstract

The NASA Glenn Research Center has developed a new Hybrid Bearing Prognostic Test Rig to evaluate the performance of sensors and algorithms in predicting failures of rolling element bearings for aeronautics and space applications. The failure progression of both conventional and hybrid (ceramic rolling elements, metal races) bearings can be tested from fault initiation to total failure. The effects of different lubricants on bearing life can also be evaluated. Test conditions monitored and recorded during the test include load, oil temperature, vibration, and oil debris. New diagnostic research instrumentation will also be evaluated for hybrid bearing damage detection. This paper summarizes the capabilities of this new test rig.

Introduction

There are numerous failure modes and failure mechanisms that may occur in complex mechanical systems. Bearing systems have been identified as a critical mechanical system with high failure rates in aerospace applications (ref. 1). Silicon nitride hybrid bearings, consisting of ceramic balls and metal races, are beginning to replace conventional bearings in special applications. Two reasons for this transition are that silicon nitride balls are about 30 percent harder and 40 percent lighter than steel. In addition, they have high wear resistance and greater corrosion resistance compared to steel balls. For high speed applications, the lower mass ceramic balls can reduce the effect of centrifugal loading, a cause of decreased fatigue life (ref. 2). Extensive resources have been invested in ceramic material development for use in new aerospace applications such as hybrid bearings. Diagnostic tools are required to decrease maintenance costs and improve safety of this enabling technology. Lack of diagnostics for ceramic/hybrid bearings is a barrier to the widespread deployment of this technology.

Development of the hybrid bearing diagnostic tools requires experimental validation of sensor technologies and analytical models to determine if failure mechanisms can be observed. The strengths, weaknesses and constraints of each measurement technology must be investigated for specific critical system failures. Accelerated component tests must be performed in a laboratory/relevant environment to assess the reliability of the diagnostic tools by identifying types of damage and failure progression rates under conditions of long-term systems degradation. The Hybrid Bearing Prognostic Test Rig will be used to perform bearing failure progression tests. The systems that show the most benefit in both safety and

on-condition maintenance will be selected for demonstration on a full scale diagnostic system for aircraft or space vehicles.

Development of generic data reduction methods and signal detection algorithms for use with real-time health monitoring systems is also required for in-space and aircraft on condition predictive maintenance. Extensive work has been performed in this area for aerospace vehicles. Empirical data combined with probabilistic methods have been used to determine the nominal statistical properties of the system, and to construct methods for the detection of anomalies and damage patterns within that framework (ref. 3).

Physics of failure models and probabilistic methods to predict bearing remaining useful life will also be developed using this test rig. Although bearings are selected based on life calculations for a specific application, the actual life achieved is affected by operation and environmental factors. Some causes of failures are inadequate lubrication and contamination. The most common failure of rolling element bearings is contact fatigue failure. This results in spalling on the inner race, outer race, and rolling elements. Once initiated the spall grows and the remaining life decreases significantly (ref. 4). Test techniques to simulate these types of failures will be developed for use during testing in the rig.

Test Facility Description and Capabilities

A schematic of the test rig is shown in figure 1. The test rig consists of a test bearing supported on a shaft by two journal wave bearings and two thrust wave bearings. Figure 2 is an expanded view of the front wave bearing assembly and test bearing. Figure 3 is an expanded view of the rear wave bearing assembly. The test bearing is loaded axially or radially with two pneumatic actuators. A 120 kW (160 HP) electric motor is used to drive the test system to 21 000 rpm.

The initial test bearings are hybrid angular contact ball bearings consisting of silicon nitride rolling elements and steel races with a bronze cage. Turbine engine oil is used to cool and lubricate the test bearings. The test bearings have an inner bore diameter of 25 mm.

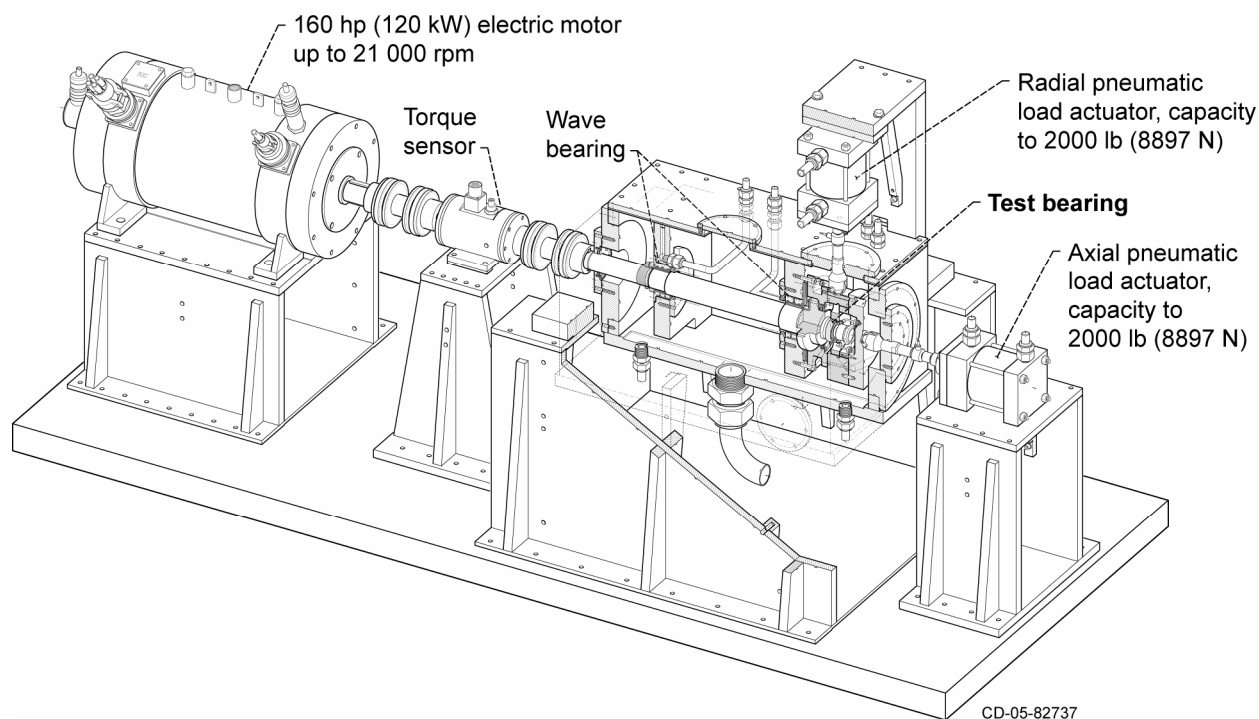


Figure 1.—Hybrid bearing prognostic test rig.

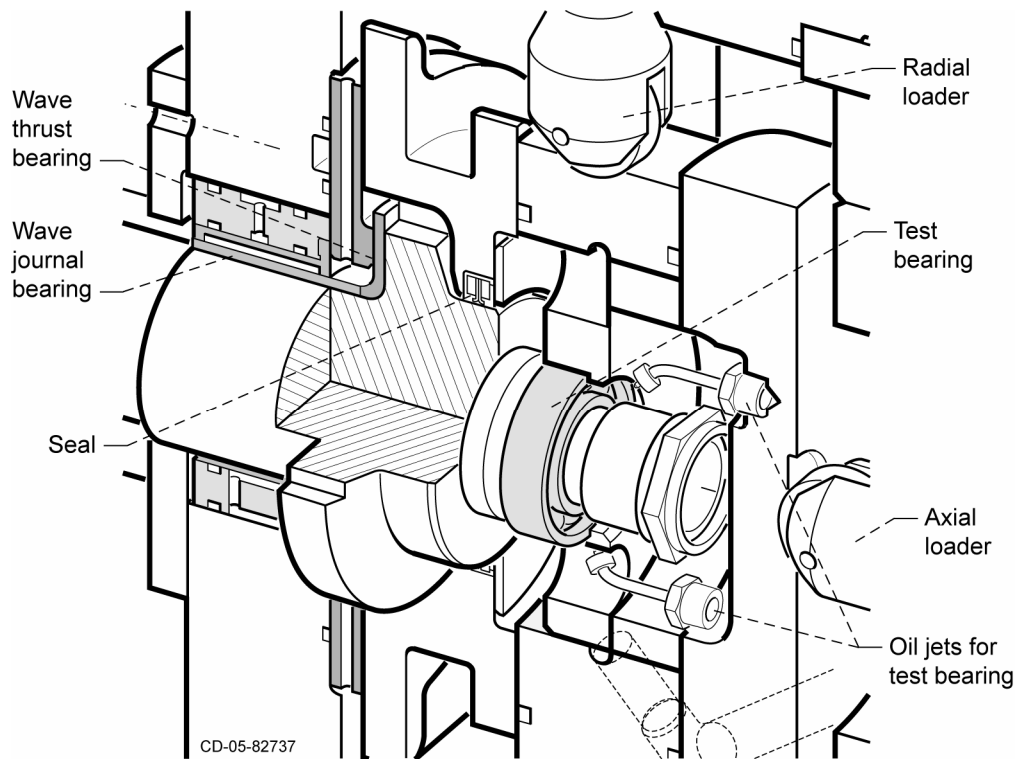


Figure 2.—Front wave bearing assembly and test bearing.

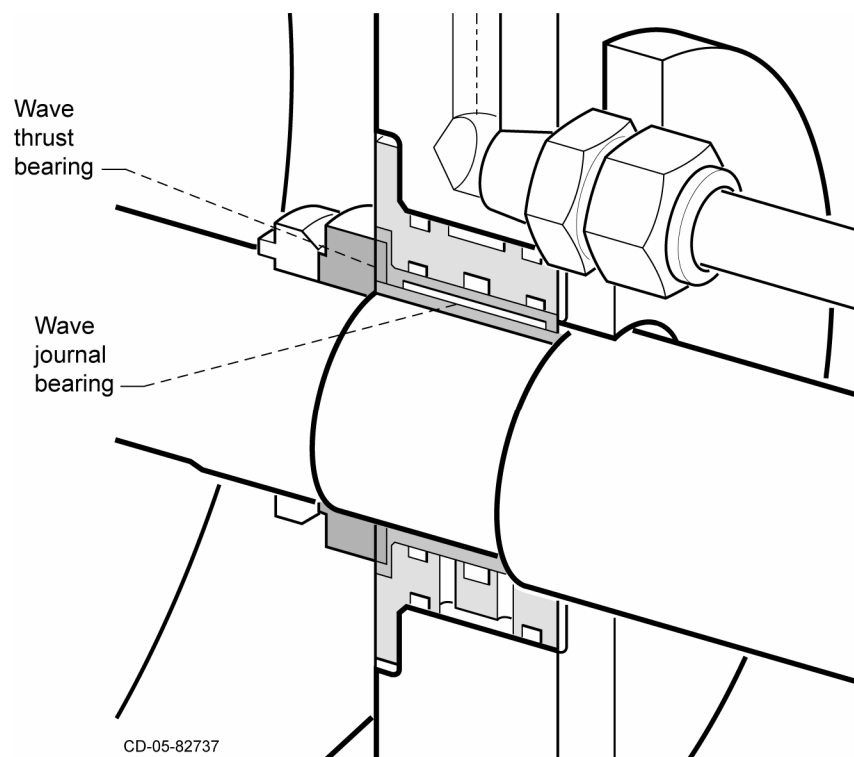


Figure 3.—Rear wave bearing assembly.

The wave bearing and test bearing each have their own lubrication systems. The lubrication systems have a 38 liter (10 gallon) reservoir, 76 liter/min (20 gpm) supply pump, and a 76 liter/min (20 gpm) scavenge pump. The reservoir has immersion heaters and an oil to water heat exchanger for controlling oil temperature. Oil temperature, pressure and flow are measured and recorded using a facility data acquisition system. Chip detectors and inductance type oil debris monitors are also installed downstream of the wave and test bearings to indicate fatigue damage when bearing debris is generated. All of the sensors are monitored and used to automatically shut down the rig if specific operational parameters are not met.

Torque required to rotate the support and test bearing is measured using an 113 N-m (1000 in.-lb) torque sensor located between the motor and rig shafts as shown on figure 1. Axial and/or radial loads on the test bearings are applied using pneumatic load actuators. Loads can be applied up to 8897 N (2000 lb) and measured with a load cell. Facility vibration data will be monitored using accelerometers located on the test rig housing.

Wave bearing technology is used in this rig for the support bearings to eliminate the vibration signature of another rolling element bearing in the test bearing spectrum. Both journal wave bearings (front and rear) have oil supply lines. Their main dimensions are listed in Table 1(a). The front thrust wave bearing (close to the test bearing) is also lubricated directly by oil supplied through its supply line. This thrust wave bearing was designed to carry a thrust load to 9000 N (2000 lb) due to the load applied to the test bearing. The rear thrust wave bearing is located on the shoulder of the wave journal bearing sleeve making a combination journal and thrust bearing assembly (ref. 5). This thrust bearing is lubricated by the oil that exits the rear wave journal bearing. The thrust wave bearing dimensions are listed in Table 1(b).

TABLE 1.—WAVE BEARING DIMENSIONS

(a) Journal wave bearing dimensions

	Front, mm	Rear, mm
Journal diameter	60	47
Journal length	40	35
Radial clearance	0.055	0.048
Wave amplitude to radial clearance ratio	0.28	0.36
Number of waves	3	3

(b) Thrust wave bearing dimensions

Thrust OD	95.3	66
Thrust ID	72	50
Thrust side clearance	0.025	0.025
Wave amplitude	0.025	0.025
Number of waves	4	4

Hard materials were selected for both the shaft and the bearing sleeve to maintain the bearing geometry under high loads. Coatings were applied to all bearing surfaces to prevent seizure and ensure a low wear rate. The wave bearing sleeve is mounted in the bearing housing that has set screws used to deform the bearing sleeve to generate the wave profile on the bearing sleeve inner diameter. All bearing parts were manufactured from VIMVAR M-50 steel. The wave profiles of the wave journal bearings were inspected and they are depicted for both front and rear bearings in figures 4(a) and (b), respectively. The position of the ports to supply the bearings with oil can also be seen in figures 4(a) and (b). The oil ports were placed symmetrical thus these wave bearings can rotate in either direction.

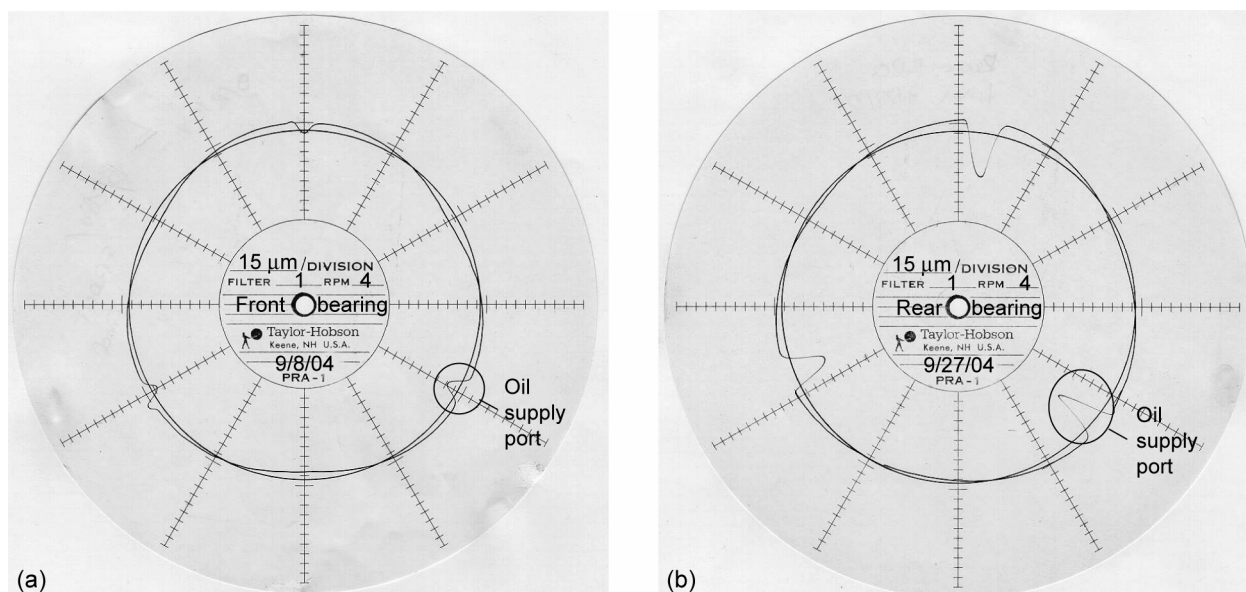


Figure 4.—Front and rear wave bearing profiles. (a) Front bearing. (b) Rear bearing.

Test Bearings

The test bearings are angular contact hybrid ball bearings. The bearing outer ring and inner ring are 52100 chrome steel. The cage material is bronze. The balls are ceramic. The test bearing dimensions are listed in Table 2. The test plan was developed by first determining the speeds and loads required to accelerate the failure of the bearings. Bearing fatigue life, L_{10} , is calculated as the minimum life in revolutions for 90 percent survival rate of a typical group of identical bearings before the area of spalling reaches 6 mm^2 (0.01 in.^2). It is given by Eq. (1), where C is the basic dynamic load rating and P is the equivalent radial load. Bearing fatigue life also refers to the number of hours at constant speed a bearing runs before fatigue is observed in the races or on the rolling element with N in rpm. Both calculations are shown in Eqs. (1) and (2).

TABLE 2.—TEST BEARING DIMENSIONS (REF. 6)

Outer ring	
OD	47 mm (1.8504 in.)
Width	12 mm (0.4724 in.)
Curvature	53 percent
Inner ring	
Bore	25 mm (0.9843 in.)
Width	12 mm (0.4724 in.)
Curvature	52 percent
Balls	
No. balls	13
Diameter	6.35 mm (0.25 in.)
Load capacity	
Dynamic	8185 N (1840 lbs)
Static radial	6334 N (1424 lbs)
Static axial	6125 N (1377 lbs)

$$L_{10} = \left(\frac{C}{P} \right)^P \times 10^6 \text{ revolutions} \quad (1)$$

$$L = \left(\frac{C}{P} \right)^P \frac{10^6}{60N} \text{ hours} \quad (2)$$

For angular contact bearings, C is calculated as the constant radial load theoretically endured for an L_{10} life of 1 million revolutions of the inner ring. The equivalent bearing load life exponent P is 3 for ball bearings. The equivalent radial load for the steel test bearings is calculated using manufacturer provided load factors and the basic dynamic load rating (ref. 6). A table of bearing fatigue life using different speeds and radial and axial loads is shown in Table 3. Initial operating parameters are highlighted. One manufacturer of hybrid rolling element bearings has performed life tests of hybrid bearings and estimates the life of hybrid bearings to be four times the life calculated based on the dynamic load rating of steel bearings (ref. 7). This would increase the number of L_{10} hours highlighted by a factor of four equal to 113 hr. The load may have to be adjusted to accelerate failures once baseline tests are performed.

TABLE 3.—TEST BEARING DIMENSIONS (REF. 6)

Thrust load, N (lb)	Radial load, N (lb)	RPM	L_{10} , hr
53 (12)	4448 (1000)	15000	72
267 (60)	↓	↓	49
445 (100)			37
890 (200)	↓		23
2669 (600)	53 (12)		31
2669 (600)	133 (30)		30
2224 (500)	267 (60)	↓	48
2224 (500)	↓	10000	71
2669 (600)		15000	28
2669 (600)	↓	10000	42

Research Diagnostic Instrumentation

Several different diagnostic tools will be used to indicate bearing failures. These include both oil based and vibration based systems. The vibration signatures during the early stages of bearing failures are often difficult to detect until localized fatigue damage occurs. For failures that do not produce localized damage, oil debris analysis will be used to detect bearing health. Vibration based diagnostic tools will be discussed first.

Vibration Based Diagnostics

Rolling element bearing fault frequencies are generated when a bearing begins to fatigue. This happens due to impulses generated when a bearing element passes the fatigue defects. The impulses occur at periodic frequencies when the bearing rotates and are often referred to as fundamental defect frequencies (ref. 8). These defect frequencies are related to bearing geometry and shaft speed. The following bearing defect frequencies in hertz were calculated for the test bearing: Ball pass frequency

outer race (BPFO); Ball pass frequency inner race (BPFI); Ball spin frequency (BSF); and Fundamental train frequency (FTF).

$$BPFI = \frac{N_b}{2} \cdot \left(1 + \frac{B_d}{P_d} \cos \theta \right) \cdot \frac{RPM}{60} \quad (3)$$

$$BPFO = \frac{N_b}{2} \cdot \left(1 - \frac{B_d}{P_d} \cos \theta \right) \cdot \frac{RPM}{60} \quad (4)$$

$$BSF = \frac{P_d}{2B_d} \cdot \left(1 - \left(\frac{B_d}{P_d} \right)^2 (\cos \theta)^2 \right) \cdot \frac{RPM}{60} \quad (5)$$

$$FTF = \frac{1}{2} \cdot \left(1 - \frac{B_d}{P_d} \cos \theta \right) \cdot \frac{RPM}{60} \quad (6)$$

Where

- N_b Number of balls or rollers
- B_d Ball or Roller diameter
- P_d Bearing Pitch Diameter
- θ Contact angle

Table 4 lists bearing defect frequencies for the test bearings at 2 speeds, 10 000 and 15 000 rpm. Several vibration based techniques exist for extracting bearing defect frequencies from vibration data. Howard (ref. 9) provides an excellent overview of vibration based diagnostic tools used to indicate bearing failures. Time domain, frequency domain, and envelope analysis techniques will be collected, monitored and processed in real-time using the data acquisition program.

TABLE 4.—BEARING DEFECT FREQUENCY COEFFICIENTS

Hertz	10000 rpm	15000 rpm
Ball pass frequency inner race (BPFI)	1268	1902
Ball pass frequency outer race (BPFO)	899	1348
Ball spin frequency (BSF)	459	688
Fundamental train frequency (FTF)	69	104

In the time domain, the vibration data waveform is analyzed for impacts that correspond to the rotation of the rolling elements past the damage for each shaft revolution. Time domain statistical parameters such as RMS, peak, crest factor, and kurtosis are calculated for a sample of time domain data. As the damage occurs, an increase in these values should occur. The bearing time domain metrics are calculated based on the following equations where \bar{x} equals the mean value of the time signal $x(t)$ having N data points:

$$peak = \frac{1}{2} \left(\max(x(t)) - \min(x(t)) \right) \quad (7)$$

$$RMS = \sqrt{\frac{1}{N} \sum_{i=1}^N (x(i) - \bar{x})^2} \quad (8)$$

$$CrestFactor = \frac{peak}{RMS} \quad (9)$$

$$Kurtosis = \frac{\frac{1}{N} \sum_{i=1}^N (x(i) - \bar{x})^4}{RMS^4} \quad (10)$$

Statistical parameters can be calculated for the entire frequency range and for user selected frequency bands.

In the frequency domain, an FFT is used to estimate the power spectrum of the discrete time signal. From the spectrum, characteristic bearing defect frequencies calculated by Eqs. (3) to (6) are identified, and the change in amplitude at these frequencies is used for trending.

Related to this is a cepstrum analysis of the vibration data. The purpose of this technique is to find repetitive impulse components in the raw vibration signal. The frequency spectrum is analyzed for frequencies that correspond to bearing defect frequency harmonics and sidebands. Cepstrum for this analysis is calculated by determining the natural logarithm of magnitude of the Fourier transform of x , then obtaining the inverse Fourier transform of the resulting sequence:

$$C(\tau) = F^{-1} \{ \log F(x(t)) \}, \text{ where } F(x(t)) \text{ is the original frequency spectrum} \quad (11)$$

Envelope analysis is another technique used during testing to indicate bearing health. Each time a defect in a rolling element makes contact with another bearing surface, an impulse is generated. The bearing structural resonances are excited by these periodic impacts at bearing defect frequencies. Enveloping isolates these small repetitive impulses and enhances the response of these small repetitive signals from the machines large low frequency synchronous vibration signals.

The technique requires the raw vibration signal to be bandpass filtered, an envelope technique applied, then an FFT signal calculated to look for bearing defect frequencies. In order to apply this technique, the vibration data is bandpass filtered around a structural resonance. Defining this filter band is one challenge of this analysis. The signal is typically bandpass filtered from 20 000 to 40 000 Hz because this range is dominated by structural resonances (ref. 9). Next, an enveloping technique is applied. This can be a squaring function or half or full wave rectification of the signal, followed by a smoothing circuit to recover the envelope signal. Then, the envelope signal is converted from the time domain to the frequency domain. The magnitude of the bearing defect frequencies is then plotted over the length of the test.

Oil Debris Diagnostics

Metallic oil debris data generated during test bearing failure will be collected with a commercially available oil debris sensor that measures the change in a magnetic field caused by passage of a metal particle. The sensor will be installed downstream of the test bearing. The amplitude of the sensor output signal is proportional to the particle mass. The sensor counts the number of particles, determines their approximate size based on user defined particle size ranges, and calculates an accumulated mass for both ferrous and nonferrous particles (ref. 10).

Electric chip detectors will also be installed downstream of the test and wave bearings to measure magnetic debris generated during bearing tests. The chip detector uses a magnet to capture debris and form an electrical bridge between contacts that indicates a state change.

An ultrasonic sensor will also be installed downstream of the test bearing. The sensor transmits acoustic pulses across the path of a liquid. Acoustic energy is then reflected off any particles encountered in the lubricant. The number of particles are counted and recorded. The sensor uses a high-frequency acoustic impulse that is reflected by both metallic and non-metallic debris particles to yield particle counts (ref. 11).

The particles generated during a component failure have features that can indicate different types of failures. Particle analysis data is available to identify fatigue wear of steel rolling element bearings. Spherical particles 1 to 5 μm are typically generated in bearing fatigue cracks prior to flat platelet fatigue particles with a 10:1 thickness ratio that are larger than 10 μm (ref. 12). Laminar particles between 20 and 50 μm with a 30:1 thickness ratio are generated through the life of the bearing, but significantly increase during fatigue damage (ref. 12). Silicon nitride rolling elements are said to fail by spalling similar to steel rolling elements (refs. 13 and 14).

A video image based diagnostic sensor will be installed downstream of the oil line to identify particle features. As particles pass in front of the camera, a picture is taken and converted to dimensional shapes and sizes. The sensor takes an image of continuous-tone (gray-scale) form and converts it to a digital form through the process of sampling and quantization. This sensor can measure both metallic and nonmetallic debris and differentiate between bubbles and air in the oil line.

Summary

The Hybrid Bearing Prognostic Test Rig has been developed to evaluate the performance health monitoring tools during the failure progression of conventional and hybrid bearings. Experiments performed in this test facility will provide valuable data on the failure progression of state-of-the-art ceramic hybrid bearings and the diagnostic tools required to predict these failures. Results from this research will enable implementation of hybrid bearings in future aerospace applications.

References

1. Merriman, T.L. and Kannel, J.W. (1999), "Bearings Chapter 14 of the NASA Space Mechanisms Handbook," Fusaro, R.L., ed., NASA TP-206988, NASA, Cleveland, OH.
2. Zaretsky, E.V. (1997), "Tribology for Aerospace Applications," *Society of Tribologists and Lubrication Engineers*, SP-37.
3. Huff, E. and Mosher, M. (2003), "An Exploration of Discontinuous Time Synchronous Averaging Using Helicopter Flight Vibration Data," *American Helicopter Society 59th Annual Forum*, Phoenix, AZ.
4. Zaretsky, E.V. (1992), "STLE Life Factors for Rolling Element Bearings," *Society of Tribologists and Lubrication Engineers*, SP-34.
5. Dimofte, F., Proctor, P., Fleming, D. and Keith, T. (2000), "Wave Fluid Film Bearing Tests for an Aviation Gearbox," NASA/TM-2000-209766, NASA, Cleveland, OH.
6. BARDEN Precision Ball Bearings Catalog CD-30 (2001), The Barden Corporation, Danbury, CT.
7. Niizeki, S. (2000), "Ceramic Bearing for Special Environments," *NSK Journal of Motion & Control*, No. 8.
8. Crawford, A.R. and Crawford, S. (1992), "The Simplified Handbook of Vibration Analysis," Computational Systems, Incorporated.

9. Howard, Ian (1994), "A Review of Rolling Element Bearing Vibration 'Detection Diagnosis and Prognosis,'" DSTO Aeronautical and Maritime Research Laboratory, DSTO-RR-0013.
10. Howe, B. and Muir, D. (1998), "In-Line Oil Debris Monitor (ODM) for Helicopter Gearbox Condition Assessment," AD-a347 503, BF Goodrich Corporation.
11. Manual for MONITEK MODEL AT3 Particle Contamination Monitor. E-mail: info@monitek.com
12. Bowen, R.E. and Westcott, V.C. (1976), "Wear Particle Atlas," Naval Air Engineering Center Contract number N00156-74-C-1682.
13. Wang, L., Snidle, R.W. and Gu, L. (2000), "Rolling Contact Silicon Nitride Bearing Technology," Wear 246 pp. 159-173.
14. Dempsey, P.J., Certo, J.M. and Morales, W. (2004), "Current Status of Hybrid bearing Damage Detection," NASA/TM-2004-212882, NASA, Cleveland, OH.

REPORT DOCUMENTATION PAGE			Form Approved OMB No. 0704-0188	
Public reporting burden for this collection of information is estimated to average 1 hour per response, including the time for reviewing instructions, searching existing data sources, gathering and maintaining the data needed, and completing and reviewing the collection of information. Send comments regarding this burden estimate or any other aspect of this collection of information, including suggestions for reducing this burden, to Washington Headquarters Services, Directorate for Information Operations and Reports, 1215 Jefferson Davis Highway, Suite 1204, Arlington, VA 22202-4302, and to the Office of Management and Budget, Paperwork Reduction Project (0704-0188), Washington, DC 20503.				
1. AGENCY USE ONLY (Leave blank)		2. REPORT DATE August 2005		3. REPORT TYPE AND DATES COVERED Technical Memorandum
4. TITLE AND SUBTITLE Hybrid Bearing Prognostic Test Rig			5. FUNDING NUMBERS WBS-22-714-90-01 1L162211A47A	
6. AUTHOR(S) Paula J. Dempsey, Joseph M. Certo, Robert F. Handschuh, and Florin Dimofte				
7. PERFORMING ORGANIZATION NAME(S) AND ADDRESS(ES) National Aeronautics and Space Administration John H. Glenn Research Center at Lewis Field Cleveland, Ohio 44135-3191			8. PERFORMING ORGANIZATION REPORT NUMBER E-15065	
9. SPONSORING/MONITORING AGENCY NAME(S) AND ADDRESS(ES) National Aeronautics and Space Administration Washington, DC 20546-0001 and U.S. Army Research Laboratory Adelphi, Maryland 20783-1145			10. SPONSORING/MONITORING AGENCY REPORT NUMBER NASA TM-2005-213597 ARL-TR-3454	
11. SUPPLEMENTARY NOTES Prepared for the 2005 Annual Meeting and Exhibition sponsored by The Society of Tribologists and Lubrication Engineers, Las Vegas, Nevada, May 15-19, 2005. Paula J. Dempsey, NASA Glenn Research Center; Joseph M. Certo and Robert F. Handschuh, U.S. Army Research Laboratory, NASA Glenn Research Center; and Florin Dimofte, University of Toledo, 2801 W. Bancroft Street, Toledo, Ohio 43606-3390. Responsible person, Paula J. Dempsey, organization code RSM, 216-433-3398.				
12a. DISTRIBUTION/AVAILABILITY STATEMENT Unclassified - Unlimited Subject Categories: 39 and 07 Available electronically at http://gltrs.grc.nasa.gov This publication is available from the NASA Center for AeroSpace Information, 301-621-0390.			12b. DISTRIBUTION CODE	
13. ABSTRACT (Maximum 200 words) The NASA Glenn Research Center has developed a new Hybrid Bearing Prognostic Test Rig to evaluate the performance of sensors and algorithms in predicting failures of rolling element bearings for aeronautics and space applications. The failure progression of both conventional and hybrid (ceramic rolling elements, metal races) bearings can be tested from fault initiation to total failure. The effects of different lubricants on bearing life can also be evaluated. Test conditions monitored and recorded during the test include load, oil temperature, vibration, and oil debris. New diagnostic research instrumentation will also be evaluated for hybrid bearing damage detection. This paper summarizes the capabilities of this new test rig.				
14. SUBJECT TERMS Rolling element bearings; Condition monitoring; Failure analysis; Fatigue; Bearings; Diagnostics; Health monitoring; Vibration; Oil debris			15. NUMBER OF PAGES 16	
			16. PRICE CODE	
17. SECURITY CLASSIFICATION OF REPORT Unclassified	18. SECURITY CLASSIFICATION OF THIS PAGE Unclassified	19. SECURITY CLASSIFICATION OF ABSTRACT Unclassified	20. LIMITATION OF ABSTRACT	

